Journal of Power Sources 193 (2009) 779–787

Contents lists available at ScienceDirect

Journal of Power Sources

journal homepage: www.elsevier.com/locate/jpowsour

Review

Life time test in direct borohydride fuel cell system

Romain Jamard [a,b,**], Jeremie Salomon [a], Audrey Martinet-Beaumont [a,*], Christophe Coutanceau [b]

[a] Commissariat à l'Energie Atomique (CEA), LITEN-DTNM-LCH, 17 av. des martyrs, 38054 Grenoble Cedex 9, France
[b] Centre National de la Recherche Scientifique (CNRS), Laboratoire de Catalyse en Chimie Organique LACCO UMR6503, 40 av. du Recteur Pineau, 86022 Poitiers, France

ARTICLE INFO

Article history:
Received 1 December 2008
Received in revised form 17 February 2009
Accepted 25 March 2009
Available online 5 April 2009

Keywords:
Anion-exchange membrane
Direct borohydride fuel cell
Life time
Permeability
Solid alkaline membrane fuel cell

ABSTRACT

The electric performances of direct borohydride fuel cells (DBFCs) are evaluated in terms of power density and life time with respect to the $NaBH_4$ concentration. A DBFC constituted of an anionic membrane, a 0.6 mg_{Pt} cm^{-2} anode and a commercial non-platinum based cathode led to performances as high as 200 mW cm^{-2} at room temperature and with natural convection of air. Electrochemical life time test at 0.55 mA cm^{-2} with a 5 M $NaBH_4$/1 M NaOH solution shows a voltage diminution of 1 mV h^{-1} and a drastic drop of performances after 250 h. The life time is twice longer with 2 M $NaBH_4$/1 M NaOH solution (450 h) and the voltage decrease is 0.5 mV h^{-1}. Analyses of the components after life time tests indicate that voltage loss is mainly due to the degradation of the cathode performance. Crystallisation of carbonate and borate is observed at the cathode side, although the anionic membrane displays low permeability to borohydride.

Contents

1. Introduction

Although DMFC and PEMFC are the most studied fuel cells, some other systems like direct borohydride fuel cell (DBFC) are emerging. It has indeed been demonstrated that good performances can be obtained with $NaBH_4$ as fuel. In 1999, Amendola et al. [1] reached 20 mW cm^{-2} at room temperature with a solid alkaline membrane fuel cell (SAMFC) equipped with an AuPt anode, fed with $NaBH_4$ liquid fuel. Since then, a lot of papers dealing with performances obtained in DBFC have been published.

A non-exhaustive review of the electric performances under different operating conditions, classified according to the nature of the anodic catalyst, is presented in Tables 1–3. Platinum-based catalysts – Pt/C [2–5,7], Pt-X alloys [1,2,6,7,29] – (Table 1) are expensive and active for the $NaBH_4$ hydrolysis reaction. Non-noble metal based catalysts (Table 2) like Au [6,8,9], Ni [10] or Pd [8,10–12] limit borohydride hydrolysis reaction. These catalysts are very interesting in order to increase the DBFC efficiency, i.e. the number of exchanged electrons for the borohydride oxidation reaction [1,13]. Catalysts based on AB_5 and AB_2 alloys [13–24] allow both direct BH_4^- oxidation and H_2 storage (Table 3). The comparison of the electric performances obtained in all these experiments is how-

* Corresponding author. Tel.: +33 438 789 190; fax: +33 438 785 117.
** Corresponding author. Tel.: +33 438 789 360; fax: +33 438 785 117.
E-mail addresses: romain.jamard@cea.fr (R. Jamard), audrey.martinent@cea.fr (A. Martinent-Beaumont).

0378-7753/$ – see front matter © 2009 Elsevier B.V. All rights reserved.
doi:10.1016/j.jpowsour.2009.03.057

Table 1
Review of performances of DBFCs fitted with anodic platinum-based catalysts under different operating conditions.

Ref.	Anode catalyst	Loading (mg cm^{-2})	Anolyte	Electrolyte	Cathode catalyst	Loading (mg cm^{-2})	Catholyte	T(°C)	Power peak
[2]	Pt/C (20%)	5	2 M $NaBH_4$ in 2 M NaOH 50 mL min^{-1}	N117	Pt/C (20%)	4	O_2 P = 2.7 atm 200 mL min^{-1}	25 °C 60 °C	20–40 mW cm^{-2} 40–70 mW cm^{-2}
	Pt-Au/C (20%)								
	Pt-Ni/C (20%)								
	Pt-Ir/C (20%)								
[3]	Pt black	5.9	0.5 M $NaBH_4$ in 6 M KOH	Liquid KOH 6 M	Pt black	6	Air (natural convection)	25 °C	44.2 mW cm^{-2}
	Pt/C (60%)	1.5							42 mW cm^{-2}
[5]	Pt/Ni	1.2	1 M $NaBH_4$ in 3 M 1 mL min^{-1}	KOH	MnO_2	3	Air (natural convection)	25 °C	19 mW cm^{-2}
[4]	Pt/C (40%)	0.4	10 wt.% $NaBH_4$ in 10 wt.% NaOH 10 mL min^{-1}	N115	Pt/C (40%)	0.4	O_2 200 mL min^{-1} (100% RH)	70 °C	120~160 mW cm^{-2}
[29]	Pt-Ru/C	1	2 M $NaBH_4$ in 1 M NaOH 2.78 mL min^{-1}	ADP-Morgane (Solvay)	Pt/C	1	O_2 0.4 mL min^{-1}	60 °C	200 mW cm^{-2}
[38]	Platinized MWCNT	0.09			Commercial Air Cathode	–			16 mW cm^{-2}
	Platinized functionalized MWCNT	0.09	10 wt.% $NaBH_4$ in 4 M NaOH	Membrane?			Air	Tamb	44.4 mW cm^{-2}
	Au-Pt/C	–							20 mW cm^{-2}
[7]	Pt/C	1.3	2 M $NaBH_4$ in 1 M NaOH	APD-Morgane (Solvay)	Air cathode	–	Air (natural convection)	Tamb	205 mW cm^{-2}
	Pt/C	0.3							70 mW cm^{-2}
	PtNi/C	0.8							120 mW cm^{-2}

ever difficult due to the very different experimental conditions: fuel concentration, electrolytes (Na^+ conductive membranes, OH^- conductive membranes [1,10,23] and alkaline solutions [3,18–20]), cathode catalysts (Pt/C, MnO_2 [5,18], Au [11,17] and metal macrocycles [7,19,20]), oxidant (air, pure O_2, and H_2O_2) and other working conditions (humidification, pressure, reactants flow rates, etc.).

Studies on DBFC are mainly devoted either to the increase of the fuel efficiency, aiming to minimize the borohydride hydrolysis reaction by using different specific catalysts [7,10,13–15,6] or to the increase of the electric performances in terms of higher achieved power density. To our knowledge, only few researches have been devoted to the stability and change in the MEAs under DBFC operating conditions. Liu et al. [13] have tested a DBFC at 200 mA cm^{-2} for 30 h. From their results, a cell voltage loss of about 2.6 mV h^{-1} could be estimated and they reported a 50% coulombic efficiency. Cheng and Scott [25] reported that a DBFC (anode Au/C//Nafion® 117//Pt/C cathode) working at 20 mA cm^{-2} underwent a voltage loss, which could be estimated from their plots to 150 mV during the first 40 h (3.75 mV h^{-1}) and 0.41 mV h^{-1} for the next 120 h. A similar behavior was observed by these authors with other anode catalysts (Ag/C, Ag/Ti, Au/C, Au/Ti) [26] and cathode catalysts (FeTMPP/C, Ag/C, Ni/C) [27]. Recently, Liu and Suda [28] have tested a DBFC at 50 mA cm^{-2} for 95 h, leading to an estimated voltage loss of 1.42 mV h^{-1} with Pt/C as cathode catalyst. Ma et al. [19] presented results recorded at the same current density showing a similar degradation rate with a very different MEA. At last, Duteanu et al. [29] presented very interesting performances obtained with a MEA (anode PtRu/C//Morgane ADP (Solvay®) membrane//Pt/C cathode) achieving a maximum power density of 200 mW cm^{-2} and life time of the MEA higher than 360 h with only 20 mV cell voltage loss.

The aim of the present work, beyond achieving high DBFC electric performance, is to study, evaluate and present the contribution of different components of a membrane electrode assembly (MEA) in DBFC electric performance and life time degradation.

2. Experimental

2.1. MEA fabrication and DBFC tests

The MEA consists basically in sandwiching a Morgane® ADP (Solvay) anion-exchange membrane between two electrodes (anode and cathode). Anodic active layer is prepared by mixing 80 wt.% of Pt/C (E-TEK 80% Pt on Vulcan XC72) and 20 wt.% of Pt black (E-TEK) in ethanol–water (1:1) and 60 wt.% PTFE emulsion in H_2O. The resulting ink is pulverized on a 3 cm × 3 cm carbon cloth in order to obtain active layers containing about 1 mg_{Pt} cm^{-2}. The commercial air cathode is based on a non-platinum active layer on Ni mesh (O'CAT® from Evionyx) [30]. Electrodes are mechanically pressed against the membrane when assembling the cell. A typical cell is presented elsewhere [7].

Aqueous solutions of 2 M, 3.5 M and 5 M $NaBH_4$ in 1 M NaOH are used for fuelling the cell using a peristaltic pump (Cole Parmer Masterflex® C/L). For life time experiments, solutions are renewed every 48 h for 2 M $NaBH_4$/1 M NaOH and every 72 h for 5 M $NaBH_4$/1 M NaOH, in order to maintain suitable $NaBH_4$ concentration. The cathode is supplied by natural air convection. All experiments are carried out at room temperature.

Electrochemical tests are carried out using an 8-channel electrochemical-regulation system (Solartron 1470 electrochemical interface) controlled by a PC with Corrware® software. *I–E* curves are recorded with a current scan rate of 2 mA s^{-1} from OCV (open circuit voltage) to 0 V. Current densities and power densities are expressed with respect the geometric surface area of electrodes, i.e. 9 cm^2. Chronopotentiometric curves are plotted at a constant current of 500 mA (i.e. 55 mA cm^{-2}). Impedance measurements are

Table 2
Review of performances of DBFCs fitted with anodic metallic non-platinum based catalysts under different operating conditions.

Ref.	Anode catalyst	Loading ($mg\,cm^{-2}$)	Anolyte	Electrolyte	Cathode catalyst	Loading ($mg\,cm^{-2}$)	Catholyte	T (°C)	Power peak
[1]	97% Au/3% Pt	–	–	AEM	Air cathode	–	Air	25 °C 70 °C	20 mW cm^{-2} 63.1 mW cm^{-2}
[10]	Ni	167		AEM	Pt/C	1			22 mW cm^{-2}
			5 wt.% $NaBH_4$ in 6N NaOH	N117 or N115	Pt/C	1	Air (natural convection)		25 mW cm^{-2}
				NRE211	Pt/C	1		25 °C	40 mW cm^{-2}
			In a static tank fuel	N112	Pt/C	1			35 mW cm^{-2}
				N112	Ag/C	1.6			33 mW cm^{-2}
[6]	Au		2 M $NaBH_4$ in 2 M NaOH				O_2		22 mW cm^{-2}
	Au-Pd	5		N117	Pt/C (20%)	4	P = 2.7 atm	60 °C	33 mW cm^{-2}
	Au-Pt		85 mL min^{-1}				200 mL min^{-1}		47 mW cm^{-2}
[9]	Ni+ . . .	14.4					Air		180 mW cm^{-2}
	. . . + Pd/C (10%)	0.6	10 wt.% $NaBH_4$ in 20 wt.% aq. NaOH	N112	Pt/C (50%)	1	5 mL min^{-1}	60 °C	250 mW cm^{-2}
	. . . + Au/C (10%)	0.6	0.15 mL min^{-1}				100%RH		195 mW cm^{-2}
	. . . + Ag/C (10%)	0.6							210 mW cm^{-2}
[8]	Au/C (10%)	0.5	25 wt.% $NaBH_4$ in 6 M NaOH	N117	Pt/C	4	1 M H_2O_2 in {1 M HCL + 3 M NaCl}	20 °C	34 mW cm^{-2}
			95 L h^{-1}				95 L h^{-1}		
[39]	Pt/C				Ir black[a]				~80 mW cm^{-2}
	Pt/C				Pd black[a]				~75 mW cm^{-2}
	Pt/C				Au/C				~50 mW cm^{-2}
	Ni on alumina silica	1	20 wt.% $NaBH_4$ in 1.8 M KOH	N112	Au/C	1	20 wt.% H_2O_2 in 5 wt.% phosphoric acid	25 °C	~12 mW cm^{-2}
	NiAl raney[a]				Au/C				~50 mW cm^{-2}
	Nb				Au/C				<10 mW cm^{-2}
	Ir black[a]				Au/C				~55 mW cm^{-2}
	Pd black				Au/C				~50 mW cm^{-2}
[11]					Pd[a]				~180 mW cm^{-2}
			10 wt.% $NaBH_4$ in 5% NaOH + 5% NH_4OH		Os[a]		10 wt.% H_2O_2 + 5 wt.% H_3PO_4		~160 mW cm^{-2}
					Au (classic)	1		Tamb	~155 mW cm^{-2}
					Ir				~130 mW cm^{-2}
	Pd (elect rodeposited)	1		N112	Pt or Rh or Ru				~110 mW cm^{-2}
					Ag				~90 mW cm^{-2}
			17 wt.% $NaBH_4$ in 5% NaOH + 5% NH_4OH		Electrodeposited Au	0.5	18 wt.% H_2O_2 + 5 wt.% H_3PO_4	26 °C	270 mW cm^{-2}
								60 °C	680 mW cm^{-2}
					Sputtered Au	0.2		26 °C	240 mW cm^{-2}
								60 °C	600 mW cm^{-2}
[12]	Ni:Pd/C:Nafion (0.75:0.3:0.1)	20	5 wt.% 20 wt.% aq. KOH 10 wt.% $NaBH_4$ in	N112	Pt/C (30%)	1	Air (natural convection)	25 °C	80 mW cm^{-2}
[25]	Au/C	2	$NaBH_4$ in 4M NaOH (static fuel tank)	N117	Pt/C	2	O_2 200 mL min^{-1}	85 °C	79 mW cm^{-2}
[28]	Ni	–	5 wt.% $NaBH_4$ in 6N NaOH	N117	Pt/XC72 (30%)	1	Air (natural convection)	25 °C	38 mW cm^{-2}
			In a static tank fuel		Ag/XC72 (20%)	1.6			32 mW cm^{-2}
[26]	Au/Ti	2	1.32 M $NaBH_4$ in 2.5 M NaOH 10 mL min^{-1}	N117	Pt/C	2	O_2	25 °C	26.8 mW cm^{-2}
	Au/Ti							85 °C	80 mW cm^{-2}
	Au/C						P amb	85 °C	70 mW cm^{-2}
	Ag/Ti						200 mL min^{-1}	85 °C	55 mW cm^{-2}
[27]	Au/C	2	1.32 M $NaBH_4$ in 2.5 M NaOH 10 mL min^{-1}	N117	Pt/C	2	O_2	85 °C	75 mW cm^{-2}
					FeTMPP/C		P amb		60 mW cm^{-2}
					Ag/C		200 mL min^{-1}		50 mW cm^{-2}
					Ni/C				40 mW cm^{-2}

[a] Unstable with fuel or oxidant.

Table 3
Review of performances of DBFCs fitted with anodic AB2 and AB5 catalysts under different operating conditions.

Ref.	Anode catalyst	Loading ($mg\,cm^{-2}$)	Anolyte	Electrolyte	Cathode catalyst	Loading ($mg\,cm^{-2}$)	Catholyte	T (°C)	Power peak
[13]	$Zr_{0.9}Ti_{0.1}Mn_{0.6}V_{0.2}Co_{0.1}Ni_{1.1}$	0.2	10 wt.% $NaBH_4$ in 20 wt.% aq. NaOH $D = 0.2\,L\,min^{-1}$	N117	Pt/C (20%)	2	O_2 $0.2\,L\,min^{-1}$ 100% RH	50 °C 70 °C 85 °C	$100\,mW\,cm^{-2}$ $140\,mW\,cm^{-2}$ $190\,mW\,cm^{-2}$
[14]	$MmNi_{3.55}A_{l0.3}Mn_{0.4}Co_{0.71}$	5	10 wt.%$NaBH_4$ in 20 wt.% aq. NaOH	N117	Pt/C (60%)	1	15 wt.% H_2O_2 pH = 1 pH = 0.5 pH = 0	 40 °C 70 °C 40 °C 70 °C 40 °C 70 °C	 $70\,mW\,cm^{-2}$ $130\,mW\,cm^{-2}$ $122\,mW\,cm^{-2}$ $256\,mW\,cm^{-2}$ $146\,mW\,cm^{-2}$ $352\,mW\,cm^{-2}$
[15]	$M_mNi_{3.55}Al_{0.3}Mn_{0.4}Co_{0.75}$ $M_mNi_{3.55}Al_{0.3}Mn_{0.4}Co_{0.75}$ $M_mNi_{4.5}Al_{0.5}$ $M_mNi_{32}Al_{0.2}Mn_{0.6}B_{0.03}Co_{1.0}$ $M_mNi_{3.2}Al_{0.2}Mn_{0.6}Co_{1.0}$ $Zr_{0.9}Ti_{0.1}Mn_{0.6}V_{0.2}Cr_{0.5}Co_{0.75}Ni_{1.2}$	5	10 wt.% $NaBH_4$ in 20 wt.% aq. NaOH $3\,mL\,min^{-1}$	N117	PtC (60%)	1	8.9 M H_2O_2 $5.5\,mL\,min^{-1}$	30 °C 70 °C 70 °C 70 °C 70 °C 70 °C	$35\,mW\,cm^{-2}$ $150\,mW\,cm^{-2}$ $130\,mW\,cm^{-2}$ $125\,mW\,cm^{-2}$ $100\,mW\,cm^{-2}$ $70\,mW\,cm^{-2}$
[16]	$Zr_{0.9}Ti_{0.1}Mn_{0.6}V_{0.2}Co_{0.1}Ni_{1.1}$ + Pd/C (10%)	–	10 wt.% $NaBH_4$ in 20 wt.% aq. NaOH $0.15\,L\,min^{-1}$	NRE-211	Pt/C (50%)	–	Air (100% RH) $5\,L\,min^{-1}$	60 °C	$290\,mW\,cm^{-2}$
[17]	$MmNi_{3.55}Al_{0.3}Mn_{0.4}Co_{0.71}$	39	4 wt.% $NaBH_4$ in 20 wt.% aq. NaOH In a static fuel tank	N961	A gold coated stainless-steel gauze	–	2 M H_2O_2 + 1.5 M H_2SO_4 + 0.1 M H_3PO_4 In a static fuel	25 °C	$50\,mW\,cm^{-2}$
[18]	$MmNi_{3.35}Al_{0.3}Mn_{0.4}Co_{0.75}$	200	0.4 g KBH_4 in 200 mL 6 M NaOH as fuel and electrolyte		MnO_2/C	2	O_2	25 °C	$70\,mW\,cm^{-2}$
[19]	$MmNi_{3.55}Co_{0.75}Mn_{0.4}Al_{0.3}$	150	$NaBH_4$ 0.8 M in 6 M NaOH as electrolyte and fuel		FePc/C	7.5	Air (natural convection)	Tamb	$92\,mW\,cm^{-2}$
[20]	$MmNi_{3.55}Co_{0.75}Mn_{0.4}Al_{0.3}$	150	$NaBH_4$ 0.8 M in 6 M NaOH as electrolyte and fuel		CoPc/C	7.5	Air (natural convection)	Tamb	$90\,mW\,cm^{-2}$
[21]	$MmNi_{3.55}Al_{0.3}Mn_{0.4}Co_{0.75}$	5	4 wt.% $NaBH_4$ in 20 wt.% aq. NaOH	N117	Prussian blue	–	2 M H_2O_2 + 1.5 M H_2SO_4 + 0.5 M KCl	Tamb	$70\,mW\,cm^{-2}$
[22]	Zr-based AB_2-type	–	10 wt.% $NaBH_4$ in 20 wt.% NaOH $25.3\,mL\,min^{-1}$ -3 °C	N115	Pt/C	–	Humidified air $10\,L\,min^{-1}$ –60 °C	76 °C	$218\,mW\,cm^{-2}$
[23]	Corrugated anode	–	10 wt.% $NaBH_4$ 20 w% NaOH, ($53\,mL\,min^{-1}$ at 35 °C	Cation-exchange membrane	Pt/C	–	Humidified air at 60 °C $10\,L\,min^{-1}$	–	$200\,mW\,cm^{-2}$
[24]	$MmNi_{3.55}Al_{0.3}Mn_{0.4}Co_{0.75}$	5	10 wt.% $NaBH_4$ in 20 wt.% aq. NaOH	N117	FeTMPP/C $PbSO_4$/C	3 8	0.5 M H_2O_2 in 0.5 M H_2SO_4	30 °C 70 °C 30 °C 70 °C	$18\,mW\,cm^{-2}$ $82\,mW\,cm^{-2}$ $32\,mW\,cm^{-2}$ $120\,mW\,cm^{-2}$

recorded using a Solartron SI 1260, controlled by Zplot® software. Electrochemical impedance of a DBFC is measured by applying a typical 10 mV AC potential excitation [31] for frequencies from 1 to 10^6 Hz. The impedance plot is performed at OCV to determine internal resistance, after the first *I–E* curve was recorded.

2.2. Characterization of the membrane properties

Ion exchange capacity (IEC) is determined by $AgNO_3$ titration. A sample of the membrane (1 cm^2) is immersed twice in about 25 mL of 1 M HCl solution during 1 h and rinsed several times in distilled water until neutral pH is obtained. The membrane is dried in an oven at 80 °C for 24 h and weighted (m_d). Finally the membrane is immersed in a 1 M HNO_3 solution (25 mL) during at least 24 h. Titration of the chloride anions in solution is made with a 0.001 M $AgNO_3$ solution using an Ag electrode (V_{eq}). The value of IEC is given by the following equation:

$$\mathrm{IEC} = \frac{V_{eq}(\mathrm{mL}) \times 0.001}{m_d(\mathrm{g})} \quad (1)$$

Same procedure than above is used to prepare the membrane and to estimate m_d for water swelling measurements. The sample is then immersed in distilled water during at least 24 h. After quickly removing water from the membrane surfaces with filter paper, the wet sample is weighted (m_w). The water uptake is given by Eq. (2):

$$G = \frac{m_w - m_d}{m_d} \quad (2)$$

Ionic conductivity of the membrane is measured by impedance using a mercury symmetric cell (Fig. 1). The mercury electrode surface is 0.283 cm^2. Resistance and ionic conductivity of the membrane is given by Eq. (3):

$$\sigma = \frac{e(\mathrm{cm})}{R(\Omega) \times S(\mathrm{cm}^2)} \quad (3)$$

2.3. Permeability measurements

A 9 cm^2 geometric surface area membrane is sandwiched at 2.5 Nm between two tanks (an anodic one with 200 mL of a 5 M $NaBH_4$/1 M NaOH solution and a cathodic one with 14 mL of a 1 M NaOH solution). After 24 h, the amount of $NaBH_4$ in the cathodic tank is determined by potassium iodide titration and by ICP-MS analysis of boron.

To simulate fuel diffusion through the membrane under conditions close to those of a working DBFC, a 9 cm^2 geometric surface area MEA is sandwiched between a cathodic compartment of the cell containing 7 mL of a 1 M NaOH O_2-saturated solution by bubbling pure oxygen at 10 mL min^{-1} and the anodic tank, as shown in Fig. 2.

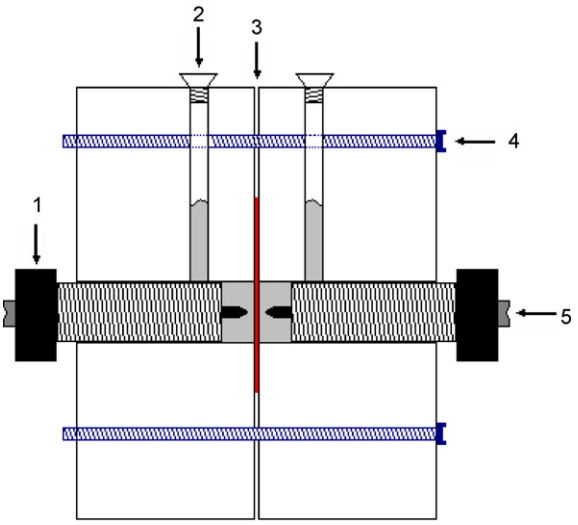

Fig. 1. Schema of the mercury cell used for impedance measurements. The membrane (3) is placed between two blocks of PMMA tightened by two nuts (4). Screws (1) serve to press mercury against the membrane and as electrical contacts (5). Mercury is put in cell via inlet (2).

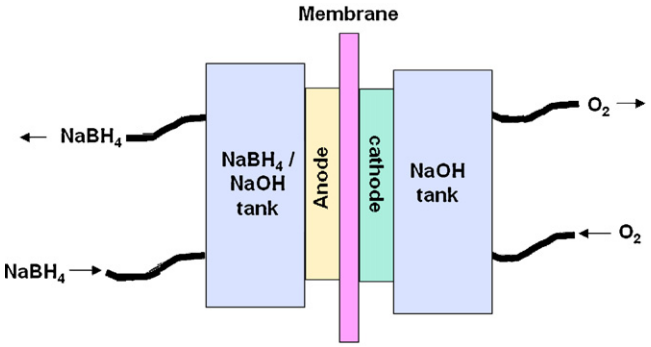

Fig. 2. Schematic representation of the cell for the permeability measurement.

3. Results and discussion

3.1. Characterization of the ADP-membrane

Table 4 presents some characteristics of the Solvay membrane used in the present studies. Its ionic conductivity is lower than that of a Nafion® membrane having the same thickness, which was measured from 50 mS cm^{-2} to 80 mS cm^{-2} [32,33]. However, these values correspond to the proton conductivity through Nafion® membranes, while in the case of a DBFC the Na^+ conductivity should

Table 4
Characterization of the properties of the Morgane® ADP-membrane (Solvay) after (t_{end}) and before (t_0) durability test for 350 h at 0.5 A, surface area of the membrane = 9 cm^2.

	Wet thickness (μm)	IEC (meq g^{-1})	Water uptake (%)	σ (mS cm^{-1})	Rint (Ω)
t_0	110	1.4	50	17.5	0.11
t_{end}	–	1.3	–	1.6	0.26

Table 5
Measurements of the membrane permeability to $NaBH_4$ under different experimental conditions.

Testing conditions	Titrimetric analysis		ICP-MS analysis	
	$NaBH_4$ (mol L^{-1})	Permeation (mol cm^{-2} s^{-1})	B (mol L^{-1})	Permeation (mol cm^{-2} s^{-1})
0 A; 24 h; 9 cm^2 (without electrodes)	3.9	7.1×10^{-8}	4.2	8×10^{-8}
0 A; 24 h; 9 cm^2	2	2.6×10^{-8}	–	–
0.25 A; 24 h; 9 cm^2	0.25	2.3×10^{-9}	1.8	2×10^{-8}
0.5 A; 24 h; 9 cm^2	0.12	1.1×10^{-9}	1.2	1×10^{-8}

be considered, which is likely lower. Table 5 exhibits results of permeation measurements. The diffusion of $NaBH_4$ through the membrane is estimated close to 7.1×10^{-8} mol cm^{-2} s^{-1}. Under the same conditions, a value of 8.2×10^{-8} mol cm^{-2} s^{-1} was measured for $NaBO_2 \cdot 4H_2O$. The diffusion of $NaBH_4$ through the membrane at OCV is three times lower: 2.6×10^{-8} mol cm^{-2} s^{-1}. The presence of the electrodes limits the fuel diffusion from the anodic side to the cathodic side. This can be explained by:

- Oxidation or hydrolyse of $NaBH_4$ on the anode catalyst.
- Low fuel diffusion through the electrodes.
- Effect of the electromotive force of the cell.
- Decrease of the osmotic pressure due to presence of dissolved oxygen, even if this contribution is probably tiny.

As soon as a current is applied to the cell, the diffusion of $NaBH_4$ through the ADP membrane is changing: it decreases from 2×10^{-8} to 1×10^{-8} mol cm^{-2} s^{-1}, with the increase of the current value from 0.25 to 0.5 A, respectively. It can also be observed that the borohydride concentration as determined by titration is lower than that from ICP-MS titration of boron. This result seems to indicate that part of borohydride has been oxidized into BO_2^- and other by-products during cell operation. Lakeman et al. [34] tested different membranes with respect to their permeability to borohydride; they found diffusion rates in the range from 1.18×10^{-6} mol cm^{-2} s^{-1} (membrane "315M") to 0.4×10^{-6} mol cm^{-2} s^{-1} (Nafion®117), i.e. at least two order of magnitude higher than that obtained with the ADP-membrane.

In conclusion, two properties of ADP membrane (conductivity and permeability) make it potentially very interesting for SAMFC application.

3.2. Electric performance of a DBFC

The concentration range of borohydride for fuel cell experiments is chosen by comparing the energy density of a DBFC with that of a Li-ion battery (200 Wh kg^{-1} [35]). The theoretical energy density of $NaBH_4$ is 9300 Wh kg^{-1}; but pure $NaBH_4$ cannot be used in a DBFC and has to be dissolved in aqueous alkaline media. Solutions containing 2 or 5 M $NaBH_4$ in 1 M NaOH correspond to about 8 wt.% or 20 wt.% in $NaBH_4$, respectively. Assuming a reasonable potential efficiency of 25%, 185 Wh kg^{-1} and 460 Wh kg^{-1} could be obtained for 2 M and 5 M $NaBH_4$, respectively. These values are equivalent or higher to those of Li-ion typical energy density.

Fig. 3 shows the polarization curves obtained with DBFC fed with different $NaBH_4$ concentrations in 1 M NaOH solutions. The OCV seems independent on borohydride concentration, remaining around 0.870–0.890 V, far from the theoretical value of the electromotive force at the equilibrium (1.64 V):

$$BH_4^- + 8OH^- \leftrightarrows BO_2^- + 6H_2O + 8e^- \quad E^\circ = -1.24\,\text{V vs. SHE} \tag{4}$$

$$O_2 + 2H_2O + 4e^- \leftrightarrows 4OH^- \quad E^\circ = 0.40\,\text{V vs. SHE} \tag{5}$$

$$BH_4^- + 2O_2 \leftrightarrows BO_2^- + 2H_2O \quad E^\circ_{\text{cell}} = 1.64\,\text{V} \tag{6}$$

According to the Nernst equation, the anodic open circuit potential (OCP) should be more negative and hence the cell OCV higher when using a more concentrated solution of $NaBH_4$:

$$E = E^\circ + \frac{RT}{nF} \ln \left[\frac{(a_{BH4^-}) \times (a_{O_2})^2}{(a_{BO_2^-}) \times (a_{H_2O})^2} \right] \tag{7}$$

It is however not the case. This is probably due to the existence of an anodic mixed potential [7], but also to the increase of the fuel crossover leading to a cathodic mixed potential.

Fig. 4 shows that anodic OCP is a little more negative when increasing $NaBH_4$ concentration. Anodic potential seems to be relatively stable with increasing the current density, with a maximum loss of 72 mV at 450 mA cm^{-2}. But this anode potential is about 300 mV more positive than the theoretical value (−1.38 mV vs. Hg/HgO). On the contrary, cathode performances were affected when increasing borohydride concentration in the anode compartment. In spite of the low permeability to $NaBH_4$ of the anionic membrane, the cathode seems to be affected by $NaBH_4$ crossover, which is responsible of the cathode potential shift towards lower values. These results are in good agreement with those of Li et al. [36].

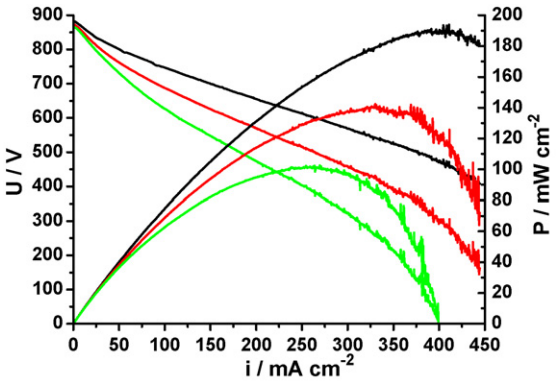

Fig. 3. Polarization and power density curves of a DBFC fed with [NaOH] = 1 mol L^{-1} and [$NaBH_4$] = 2 mol L^{-1} (in black), [$NaBH_4$] = 3.5 mol L^{-1} (in red) and [$NaBH_4$] = 5 mol L^{-1} (in green). Anode: 0.6 mg_{Pt} cm^{-2} – anion exchange membrane (AEM) Morgane® ADP – air cathode O'CAT® from Evionyx; current scan rate = 2 mA s^{-1}, room temperature, D_{NaBH_4} = 10 mL min^{-1}, natural air convection (For interpretation of the references to color in this figure legend, the reader is referred to the web version of the article).

BH_4^- spontaneous hydrolysis can occur following the chemical reactions described in Eqs. (8)–(10):

$$BH_4^- + H_2O \leftrightarrows BH_3(OH)^- + H_2 \tag{8}$$

$$BH_3(OH)^- + H_2O \leftrightarrows BO_2^- + 3\,H_2 \tag{9}$$

$$BH_4^- + 2\,H_2O \leftrightarrows BO_2^- + 4\,H_2 \tag{10}$$

As a consequence, competitive oxidation of H_2 and BH_4^- can occur at the anode catalyst surface. In that case, Eq. (4) becomes:

$$BH_4^- + xOH^- \leftrightarrows BO_2^- + (x-2)H_2O + xe^- + \left(4 - \frac{x}{2}\right) H_2 \tag{11}$$

Fig. 5 presents the H_2 evolution flow rate at the anode measured during the electrochemical tests presented in Fig. 3. Theoretical H_2 evolution flows are also reported for $x = 2$, $x = 4$ and $x = 6$ in Eq. (11).

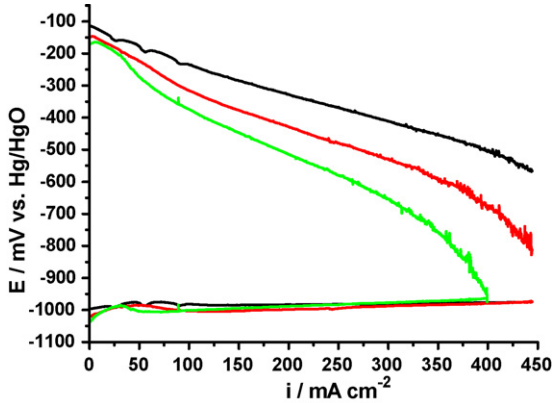

Fig. 4. Anodic and cathodic potentials, expressed in mV vs. Hg/HgO reference, as a function of the applied current density. Experimental conditions are those used in Fig. 3.

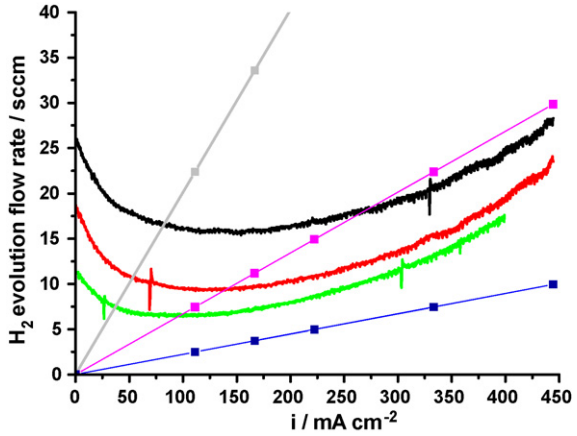

Fig. 5. H_2 evolution flow rate, expressed in sccm (standard cubic centimeters per minute), obtained during polarization curves. Theoretical H_2 evolution flows for $x = 2$ (grey), $x = 4$ (purple) and $x = 6$ (blue) in Eq. (11) Experimental conditions are those used in Fig. 3 (For interpretation of the references to color in this figure legend, the reader is referred to the web version of the article).

H_2 evolution already occurs at the anode OCP, which is likely due to spontaneous hydrolysis of $NaBH_4$, a side reaction affecting the borohydride efficiency use, and then the faradic efficiency of the cell. H_2 evolution is strongly dependent on the borohydride concentration. The higher the concentration is, the lower its value is. According to studies and data from Li et al. [9], the following interpretation could be proposed: hydrogen evolution decreases from ocp to a minimum which depends on borohydride concentration, at ocp, only $NaBH_4$ hydrolysis reaction occurs on the catalytic sites; as soon as a current is generated, competition between three reactions starts to take place at the catalyst surface: $NaBH_4$ hydrolysis reaction, $NaBH_4$ oxidation reaction and H_2 oxidation reaction. On a Pt/C catalyst, kinetics favor hydrogen oxidation reaction compared to $NaBH_4$ oxidation reaction, which leads to decrease the number of available catalytic sites for $NaBH_4$ hydrolysis reaction. As a consequence, the hydrogen flow rate decreases. After reaching a minimum, hydrogen evolution increases with current density. In higher current density range, the turn-over of BH_4^- on catalytic sites and its oxidation rate is increased, involving in the same time the increase of the H_2 evolution rate; hydrogen is then more rapidly formed than it is consumed. According to Eq. (11), the amount of hydrogen produced is a linear function of the number of electrons involved in the $NaBH_4$ oxidation process. The latter could then be calculated, and was found to be close to 4, whatever the BH_4^- concentration. All results and data concerning the DBFC are summarized in Table 6. It is also interesting to remark that internal resistance of the fuel cell is dependant on $NaBH_4$ concentration, which probably could be explained by the increase of viscosity of the fuel solution. Our DBFC system, working at room temperature where only natural air convection is used to feed the cathode, leads to electrical performance in the range from 100 to 200 mW cm^{-2}, according to the borohydride concentration. This is higher than performance given by other authors under equivalent working conditions (about 90 mW cm^{-2} [19,20]). However, Gu et al. [11] claimed achieving 600 mW cm^{-2} with optimized operating conditions and electrodes.

Table 6
Experimental conditions and results concerning DBFCs electrical performance measurements.

C_{NaBH_4}, mol L^{-1}	2	3.5	5
C_{NaOH}, mol L^{-1}	1.0	1.0	1.0
OCV, V	0.886	0.879	0.871
R, Ω	0.097	0.115	0.123
P_{max}, mW cm^{-2}	194	140	103
OCP, V vs. Hg/HgO	−0.996	−1.022	−1.037
E_{anode}, V vs. Hg/HgO at 450 mA cm^{-2}	−0.974	−0.975	−0.965
Initial H_2 evolution, sscm	25.5	19	11.5
H_2 evolution, sscm at 450 mA cm^{-2}	29	24.5	17.5

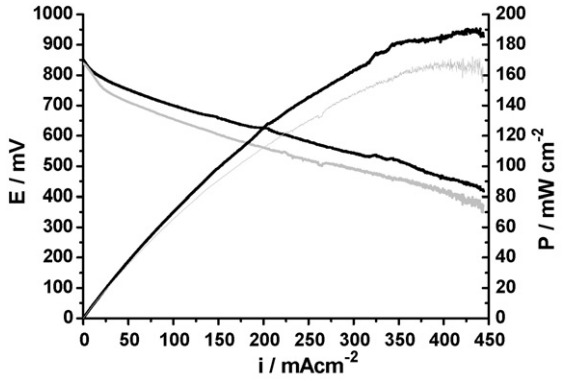

Fig. 6. Polarization and power density curves of a DBFC fed with [$NaBH_4$] = 2 mol L^{-1} in [NaOH] = 1 mol L^{-1} (black line) and [$NaBH_4$] = 5 mol L^{-1} in [NaOH] = 1 mol L^{-1} (grey line). Black lines: anode 1 mg_{Pt} cm^{-2} – AEM: Morgane® ADP – air cathode O'CAT® from Evionyx; grey lines: anode: 1.9 mg_{Pt} cm^{-2} – AEM: Morgane® ADP – air cathode O'CAT® from Evionyx; current scan rate: 2 mA s^{-1}, room temperature, D_{NaBH_4} = 10 mL min^{-1}, natural air convection.

3.3. Life time tests

Fig. 6 presents the polarization curves of two direct borohydride fuel cells fed with 2 M $NaBH_4$/1 M NaOH and 5 M $NaBH_4$/1 M NaOH. In both cases, the maximum power density is achieved at about 450 mA cm^{-2}: 170 mW cm^{-2} with 5 M $NaBH_4$ against 190 mW cm^{-2} with 2 M $NaBH_4$.

Chronopotentiometric studies have been carried out at 0.5 A (55 mA cm^{-2}), at room temperature, with natural convection of air, and with fuel recirculation (Fig. 7); the fuel tank is regularly refilled to avoid problems associated with BH_4^- concentration depletion and capacity loss. Considering a theoretical 8 electrons process, 200 mL of solutions of 2 or 5 M $NaBH_4$ in 1 M NaOH corresponds to a capacity of 86 or 214, Ah respectively. By refilling the solutions each 24 or 48 h, the total capacity decreases are only 14% and 12%, respectively. Therefore, it can be assumed that no significant cell voltage loss occurs due to decrease of $NaBH_4$ concentration in the course of the experiments.

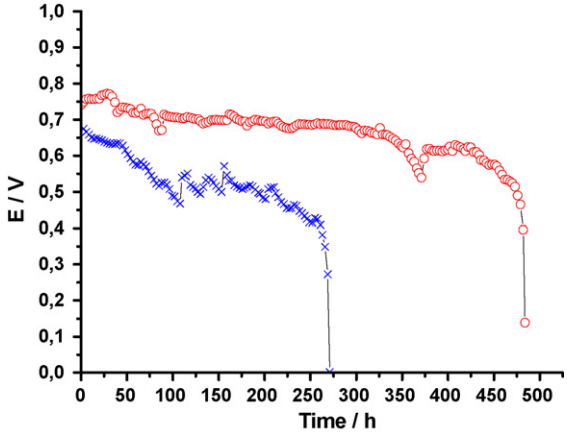

Fig. 7. Chronopotentiometric curves obtained with both DBFCs fed with 2 M $NaBH_4$/1 M NaOH (circles) and with 5 M $NaBH_4$/1 M NaOH (crosses). I = 0.5 A, S = 9 cm^2. Experimental conditions are those used in Fig. 6.

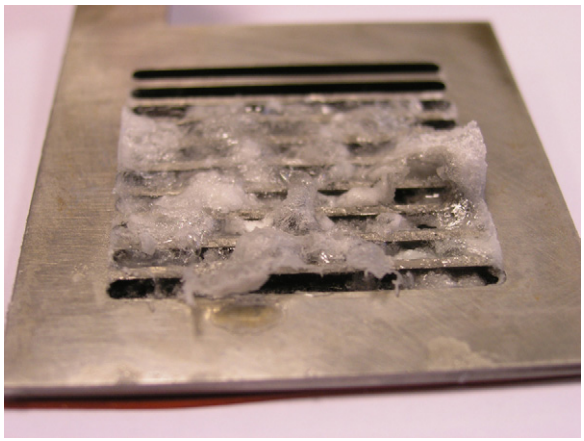

Fig. 8. Photograph of the air cathode current collector after long term test realized in Fig. 7.

Lifespan of about 475 h was observed with 2 M $NaBH_4$/1 M NaOH fuel, whereas it decreases down to 275 h with 5 M $NaBH_4$. Moreover, the cell voltage is at least 100 mV lower with the higher concentrated solution during all the test duration. Voltage losses of 0.5 and 1 mV h^{-1} are recorded with 2 M $NaBH_4$/1 M NaOH and with 5 M $NaBH_4$/1 M NaOH, respectively. These values are slightly lower than those obtained with a Na^+ exchange membrane (Nafion® 117) for the same current density [27,28], but higher than those obtained by other authors with similar hydroxyl exchange membrane [26]. The electrochemical performance degradation, characterized by the voltage loss of the cell, is partly related to fuel crossover. After electrochemical experiments, it was observed that the cathodic collector was covered by a whitish material (Fig. 8). Characterizations of this material by IR spectroscopy and X-ray scattering (Fig. 9) showed the presence of sodium borate, sodium borohydride and sodium carbonate. As the diffusion of $NaBH_4$ and $NaBO_2$ through the membrane occurs with the same rate, it is not surprising to have these two products at the cathode. Sodium borate could be produced either at the anode or at the cathode; however, the cathode catalyst appears to be relatively tolerant to the presence of borohydride. Therefore, borates are likely mainly produced at the anode. Anyway, the final result is that those by-products represent an additional barrier to the O_2 diffusion. The presence of sodium borohydride could also be at the origin of a mixed potential at the cathode, which also can explain a part of the voltage loss during the long term test. The carbonates come from the reaction of air CO_2 with sodium hydroxide and could be also an extra barrier to the O_2 diffusion in the air cathode.

A specific study has been carried out on 4 MEAs with 5 M $NaBH_4$/1 M NaOH in order to confirm the origin of the cell performance degradation. The MEAs were maintained at 0.5 A until the DBFC voltage falls down to 0. Then, a regenerative treatment is applied for each of them: (i) for all MEAs, rinsing of the electrodes and membrane several times with distilled water, (ii) for MEA2 and MEA4, the membrane is dipped in a 1 M NaOH solution for 12 h, (iii) for MEA3 and MEA4, a new cathode is used. Each treated MEA is again tested at 0.5 A. Time of "resurrection" indicates the additional period after the regenerative treatment, during which the fuel cell voltage is superior to 0. The duration of these periods are presented in Fig. 10. For MEA1, the "resurrection" time is very short (less than 20 h); it becomes twice higher when the membrane is dipped in 1 M NaOH (MEA2). Comparing MEA3 and MEA4, the same effect can be observed. The replacement of the cathode has a more important impact on the "resurrection" time: when comparing MEA1 and MEA3 in one hand and MEA2 and MEA4 in the other hand, it is multiplied by a factor close to 4. The cathode appears then as the key point of cell performance degradation, likely due to borohydride and oxidation by-products crossover. However, the degradation of membrane performance is not negligible. It is proposed that the following degradation processes occur:

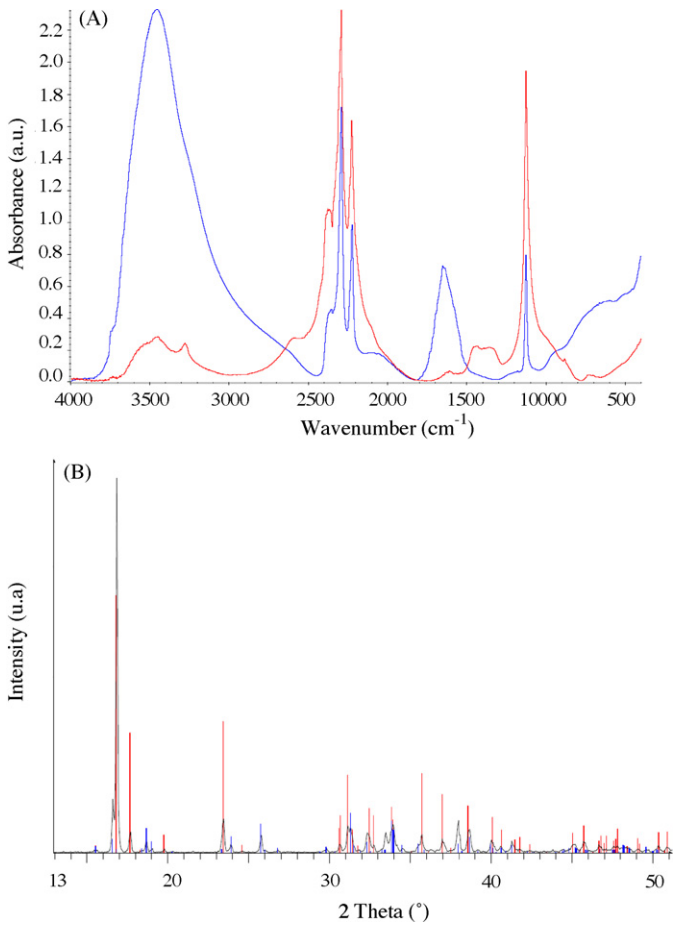

Fig. 9. Analyses of the whitish material obtain at the cathode after long term test; (A) IR spectra of the product (blue line) and of pure $NaBH_4$ (red line) recorded in the 500–3000 cm^{-1} range. (B) X-ray diffraction patterns of the product (black line), pure $NaB(OH)_4$ (blue line) and pure $NaB(OH)_4$, $2H_2O$ (red line) (For interpretation of the references to color in this figure legend, the reader is referred to the web version of the article).

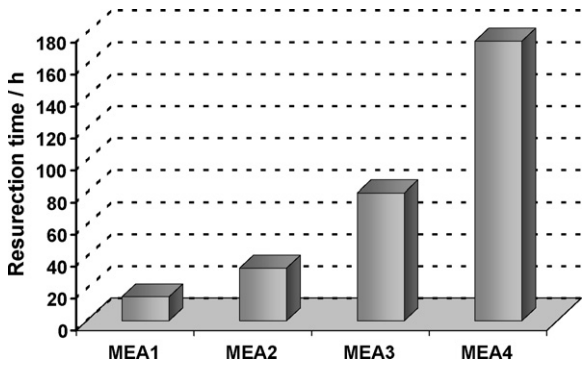

Fig. 10. "Resurrection" time at 0.5 A after to regeneration treatment on MEAs. MEA1: rinsing with distilled water; MEA2: rinsing with distilled water and dipping of the membrane in a 1 M NaOH solution for 12 h; MEA3: rinsing with distilled water and replacement of the cathode; MEA4: rinsing with distilled water, dipping of the membrane in a 1 M NaOH solution for 12 h and replacement of the cathode. Experimental conditions are the same as in Fig. 6.

- Degradation of the cathode architecture and material (catalyst is probably not as stable as expected).
- Pollution of cathodic catalytic sites by the fuel and its by-products.
- Saturation of the cationic sites of the membrane by BH_4^- and/or BO_2^-, which limits conduction of hydroxides and could explain the decrease of conductivity while IEC displays only a little decrease after 350 h (Table 4).
- Precipitation of the fuel in the cationic sites could also occur, leading to block the pores of the electrode and to reduce the electrode "breathing".

In addition, a slight elution of the anode catalyst could lead to a slow decrease of the cell performances. However, good cell performances are not recovered when the anode is replaced by a new one, conversely to what was observed by replacing the cathode. With a more concentrated solution these phenomena will be probably more premature due to the increase of BH_4^- or/and BO_2^- crossover which are suspected to be at the origin of materials degradations (membrane and cathode especially) and lead to a less important life time. These results lead us to focus in the future on the degradation process of the cathodic side. Catalyst change has notably to be considered more particularly by evaluating the specific area change using cyclic voltametry method and estimating particles agglomeration by TEM.

4. Conclusions

SAMFCs are very attractive with respect to the low cost of materials (membrane, non-noble catalyst and collector) and are at the beginning of their development. The DBFC presents really good power performances compared with other direct liquid fuel cells, although lifespan has to be enhanced. Electrochemical life time tests at 0.55 A cm^{-2} of a DBFC fed with a 5 M $NaBH_4$/1 M NaOH solution displayed a drastic drop of performances after 250 h. The life time was twice longer with 2 M $NaBH_4$/1 M NaOH solution. It seems that voltage loss is mainly due to the degradation of the cathode, while the membrane and the anode play a less important role in performance degradation. Crystallisation of carbonate and borate is observed at the cathodic side, although Morgane ADP anionic membrane displays low permeability to borohydride. How could it be circumvented? Membrane post treatment could be envisaged [37] to limit fuel crossover.

Another key point is the fuel efficiency. It is very important to develop anodic catalysts allowing an 8 electrons process or the total oxidation of the released H_2 by borohydride hydrolyse at a given working point. This aspect will be treated in a next article.

Acknowledgements

Authors are grateful to Solvay S.A. for providing anionic membranes and for financial support. They acknowledge the French Ministry of Research for financial contribution.

References

[1] S. Amendola, P. Onnerud, M. Kelly, P. Petillo, S. Sharp-Goldman, M. Binder, J. Power Sources 84 (1999) 130.
[2] E. Gyenge, M. Atwan, D. Northwood, J. Electrochem. Soc. 153 (2006) A150.
[3] J.-H. Kim, H.-S. Kim, Y.-M. Kang, M.-S. Song, S. Rajendran, S.-C. Han, D.-H. Jung, J.-Y. Lee, J. Electrochem. Soc. 151 (2004) A1039.
[4] Ki Tae Park, Un Ho Jung, Seong Uk Jeong, Sung Hyun Kim, J. Power Sources 162 (2006) 192.
[5] A. Verma, A.K. Jha, S. Basu, J. Power Sources 141 (2005) 30.
[6] M.H. Atwan, C.L.B. Macdonald, D.O. Northwood, E.L. Gyenge, J. Power Sources 158 (2006) 36.
[7] R. Jamard, A. Latour, J. Salomon, P. Capron, A. Martinent-Beaumont, J. Power Sources 172 (2008) 287.
[8] C. Ponce de León, F.C. Walsh, A. Rose, J.B. Lakeman, D.J. Browning, R.W. Reeve, J. Power Sources 164 (2007) 441.
[9] Z.P. Li, B.H. Liu, J.K. Zhu, S. Suda, J. Power Sources 163 (2006) 555.
[10] B.H. Liu, Z.P. Li, K. Arai, S. Suda, Electrochim. Acta 50 (2005) 3719.
[11] L. Gu, N. Luo, G.H. Miley, J. Power Sources 173 (2007) 77.
[12] B.H. Liu, Z.P. Li, S. Suda, J. Power Sources 175 (2008) 226.
[13] B.H. Liu, Z.P. Li, Se. Suda, J. Electrochem. Soc. 150 (2003) A868.
[14] R.K. Raman, N.A. Choudhury, A.K. Shukla, Electrochem. Solid-State Lett. 7 (2004) A488.
[15] N.A. Choudhury, R.K. Raman, S. Sampath, A.K. Shukla, J. Power Sources 143 (2005) 1.
[16] Z.P. Li, B.H. Liu, K. Arai, S. Suda, J. Alloy Compd. 404–406 (2005) 648.
[17] R.K. Raman, S.K. Prashant, A.K. Shukla, J. Power Sources 162 (2006) 1073.
[18] Y.-G. Wang, Y.-Y. Xia, Elecrochem. Commun. 8 (2006) 1775.
[19] J. Ma, J. Wang, Y. Liu, J. Power Sources 172 (2007) 220.
[20] J. Ma, Y. Liu, P. Zhang, J. Wang, Electrochem. Commun. 10 (2008) 100.
[21] G. Selvarani, S.K. Prashant, A.K. Sahu, P. Sridhar, S. Pitchumani, A.K. Shukla, J. Power Sources 178 (2008) 86.
[22] C. Kim, K.-J. Kim, M.Y. Ha, J. Power Sources 180 (2008) 154.
[23] C. Kim, K.-J. Kim, M.Y. Ha, J. Power Sources 180 (2008) 114.
[24] R.K. Raman, A.K. Shukla, J. Appl. Electrochem. 35 (2005) 1157.
[25] H. Cheng, K. Scott, J. Power Sources 160 (2006) 407.
[26] H. Cheng, K. Scott, J. Appl. Electrochem. 36 (2006) 1361.
[27] H. Cheng, K. Scott, J. Electroanal. Chem. 596 (2006) 117.
[28] B.H. Liu, S. Suda, J. Power Sources 164 (2007) 100.
[29] N. Duteanu, G. Vlachogiannopoulos, M.R. Shivhare, E.H. Yu, Keith Scott, J. Appl. Electrochem. 37 (2007) 1085.
[30] http://www.evionyx.com/pdfs/o_cat.pdf.
[31] L. Géniès, Y. Bultel, R. Faure, R. Durand, Electrochim. Acta 48 (2003) 3879.
[32] K.M. Halim, F.N. Buchi, O. Haas, M. Stamm, G.G. Sherer, Electrochim. Acta 39 (1994) 1303.
[33] S.W. Choi, Y.-Z. Fu, Y.R. Ahn, S.M. Jo, A. Manthiram, J. Power Sources 180 (2008) 167.
[34] J.B. Lakeman, A. Rose, K.D. Pointon, D.J. Browning, K.V. Lovell, S.C. Waring, J.A. Horsfall, J. Power Sources 162 (2006) 765.
[35] M. Broussely, G. Archdale, J. Power Sources 136 (2004) 386.
[36] Z.P. Li, B.H. Liu, K. Arai, K. Asaba, S. Suda, J. Power Sources 126 (2004) 28.
[37] M. Schieda, S. Roualdès, J. Durand, A. Martinent, D. Marsacq, Desalination 199 (2006) 286.
[38] K. Deshmukh, K.S.V. Santhanam, J. Power Sources 159 (2) (2006) 1084.
[39] G.H. Miley, N. Luo, J. Mather, R. Burton, G. Hawkins, L. Gu, E. Byrd, R. Gimlin, P.J. Shrestha, G. Benavides, J. Laystrom, D. Carroll, J. Power Sources 165 (2) (2007) 509.